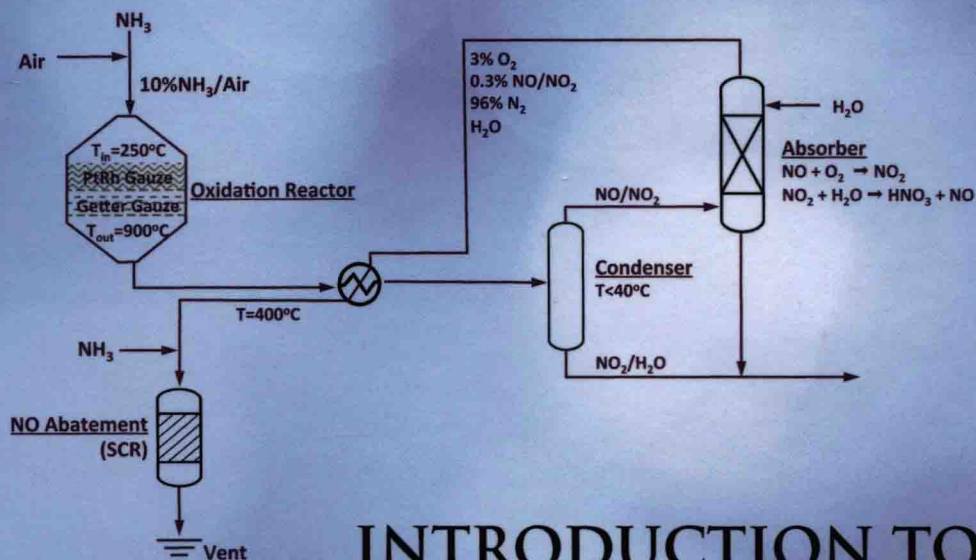


ROBERT J. FARRAUTO  
LUCAS DORAZIO  
C. H. BARTHOLOMEW



# INTRODUCTION TO CATALYSIS AND INDUSTRIAL CATALYTIC PROCESSES

---

# *INTRODUCTION TO CATALYSIS AND INDUSTRIAL CATALYTIC PROCESSES*

**ROBERT J. FARRAUTO**

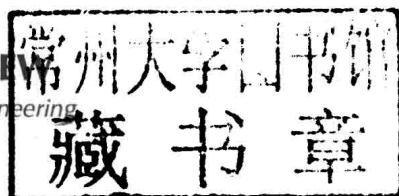
*Earth and Environmental Engineering Department  
Columbia University  
New York, New York*

**LUCAS DORAZIO**

*BASF Corporation  
Iselin, New Jersey*

**C.H. BARTHOLOMEW**

*Department of Chemical Engineering  
Brigham Young University  
Provo, Utah*



**AIChE**   
The Global  
Home of  
Chemical Engineers

**WILEY**

Copyright © 2016 by John Wiley & Sons, Inc. All rights reserved.

A joint publication of the American Institute of Chemical Engineers, Inc. and John Wiley & Sons, Inc.

Published by John Wiley & Sons, Inc., Hoboken, New Jersey.

Published simultaneously in Canada.

No part of this publication may be reproduced, stored in a retrieval system, or transmitted in any form or by any means, electronic, mechanical, photocopying, recording, scanning, or otherwise, except as permitted under Section 107 or 108 of the 1976 United States Copyright Act, without either the prior written permission of the Publisher, or authorization through payment of the appropriate per-copy fee to the Copyright Clearance Center, Inc., 222 Rosewood Drive, Danvers, MA 01923, (978) 750-8400, fax (978) 750-4470, or on the web at [www.copyright.com](http://www.copyright.com). Requests to the Publisher for permission should be addressed to the Permissions Department, John Wiley & Sons, Inc., 111 River Street, Hoboken, NJ 07030, (201) 748-6011, fax (201) 748-6008, or online at <http://www.wiley.com/go/permission>.

**Limit of Liability/Disclaimer of Warranty:** While the publisher and author have used their best efforts in preparing this book, they make no representations or warranties with respect to the accuracy or completeness of the contents of this book and specifically disclaim any implied warranties of merchantability or fitness for a particular purpose. No warranty may be created or extended by sales representatives or written sales materials. The advice and strategies contained herein may not be suitable for your situation. You should consult with a professional where appropriate. Neither the publisher nor author shall be liable for any loss of profit or any other commercial damages, including but not limited to special, incidental, consequential, or other damages.

For general information on our other products and services or for technical support, please contact our Customer Care Department within the United States at (800) 762-2974, outside the United States at (317) 572-3993 or fax (317) 572-4002.

Wiley also publishes its books in a variety of electronic formats. Some content that appears in print may not be available in electronic formats. For more information about Wiley products, visit our web site at [www.wiley.com](http://www.wiley.com).

***Library of Congress Cataloging-in-Publication Data:***

Names: Farrauto, Robert J., 1941- author. | Dorazio, Lucas, author. |

Bartholomew, C. H., author.

Title: Introduction to catalysis and industrial catalytic processes / Robert

J. Farrauto, Lucas Dorazio, C. H. Bartholomew.

Description: Hoboken : John Wiley & Sons, Inc., 2016. | Includes index.

Identifiers: LCCN 2015042209 (print) | LCCN 2015044585 (ebook) | ISBN

9781118454602 (cloth) | ISBN 9781119089155 (pdf) | ISBN 9781119101673 (epub)

Subjects: LCSH: Catalysis.

Classification: LCC QD505 .F37 2016 (print) | LCC QD505 (ebook) | DDC

660/.2995-dc23

LC record available at <http://lcn.loc.gov/2015042209>

Printed in the United States of America.

10 9 8 7 6 5 4 3 2 1

*INTRODUCTION  
TO CATALYSIS  
AND INDUSTRIAL  
CATALYTIC PROCESSES*



*To my wife Olga (Olechka) who has been a partner, friend, and critic over the precious years we have been together. She has provided love, understanding, focus, and a new vision to life. I thank my loving daughters, Jill Marie and Maryellen, and their husbands Glenn and Tom. I am fortunate to have inspiring grandchildren Nicky, Matt, Kevin, Jillian, Owen, and Brendan and stepdaughters Elena and Marina. I want to acknowledge my brother John (wife Noella) and sister Marianna (husband Ron) who have supported me emotionally through all of our years together. I am forever grateful to my parents who raised me as a proud Italian-American with a desire to help others.*

**Robert J. Farrauto**

*To my wife Cara, whose encouragement and support helped complete this project, and to my young children Lauren and Zach for their support and genuine interest in my career.*

**Lucas Dorazio**

*To my loving wife, friend, and critic, Karen, of over 49 years, who has supported me in all good things and forgiven my faults and mistakes; my 5 children and 10 grandchildren who have brought me mostly joy, been a constant source of fun and entertainment, and have given me understanding, support, love, excitement, inspiration, and challenges that have led to my growth; my loving, supportive brothers and sisters (all 7); and my dad and mom who taught me to love learning, life, and the Christian way. I especially dedicate this work (an offspring of our earlier book) to my son Charles who died unexpectedly on September 25, 2014 and who greatly touched and brightened the lives of his family, friends, and coworkers.*

**Calvin H. Bartholomew**



---

# PREFACE

"Simplicity is the ultimate sophistication."

**T**HESE WORDS of Leonardo da Vinci were recently quoted by Steve Jobs of Apple in the book by Walter Isaacson. *Simplicity* was the first guiding principle in the preparation of this introductory book. The second guiding principle was to *share our considerable industrial and academic experience* in working with and teaching about catalysis fundamentals and industrial catalytic processes.

All of us authors have worked in industry and academia, two of us as technical consultants. Dr. Farrauto was affiliated with BASF (formerly Engelhard), Iselin, New Jersey for 37 years having worked in environmental, chemical, petroleum, and alternative energy fields and is now Professor of Practice in the Earth and Environmental Engineering Department at Columbia University in the City of New York. Dr. Dorazio, a research engineer at BASF (New Jersey), has worked in catalysis research and in scale-up of catalysts for the chemical, petroleum, and environmental fields. He is also Adjunct Professor in the Chemical Engineering Department at New Jersey Institute of Technology (NJIT). Dr. Bartholomew, Professor Emeritus in the Chemical Engineering Department at Brigham Young University, Provo, Utah, worked for a year at Corning Glass (with Dr. Farrauto) in auto emissions control after which he taught and conducted research and consulting for 41 years in catalyst design/deactivation and reactor/process design for environmental cleanup and synthetic fuel production. He continues to be active in writing, teaching short courses, and consulting. All of us have been widely engaged in various degrees of teaching industrial catalysis at the undergraduate and graduate levels. Bartholomew and Farrauto have coauthored the widely used text and reference book entitled "Fundamentals of Industrial Catalytic Processes," a more advanced, in-depth version of the topics in the current book and a likely sequel to this book.

Industrial catalytic applications are seldom taught in undergraduate chemistry and chemical engineering programs, a surprising fact, given the large number of commercial processes that utilize catalysis. Thus, we accepted the challenge of writing a book that would introduce senior level undergraduates and new graduate students to this exciting field of catalytic processes, which is fundamental to chemical engineering and chemistry as practiced in industry. The need for a thorough understanding of fundamental principles of chemistry and catalysis is given. The transition of this knowledge to their commercial applications is our objective, especially for the many chemistry and chemical engineering students who spend much of their careers working in industry with catalytic processes. We also include the many professionals of varying disciplines



who suddenly find themselves with a new assignment of working on a catalytic process without previous training in the basics of catalysis and catalytic processes.

Our goal is to explain the fundamental principles of catalysis and their applications of catalysis in a simple, introductory textbook that excites those contemplating an industrial career in chemical, petroleum, alternative energy, and environmental fields in which catalytic processes play a dominant role. The book focuses on non-proprietary, basic chemistries and descriptions of important, currently used catalysts and catalytic processes. Considerable practical examples, recommendations, and cautions located throughout the book are based on authors' experience gleaned from teaching, research, commercial development, and consulting, including feedback from many students and associates. Suggested readings (reviews, books, and journal articles) are included at the end of each chapter to encourage interested readers to deepen their knowledge of these topics. Process diagrams have been simplified to provide an overview of principal process units (e.g., reactors and separation units) and important process steps, including reactant and product streams. Nevertheless, it should be recognized that commercial engineering process flow sheets include many other details and specifications, for example, piping, pumps, valves, heat exchangers, and other process equipment needed to operate and control the plant, including special equipment for plant start-up, catalyst pretreatment, purges, safety, regeneration, and so on.

Chapters 1–5 introduce the reader to basic principles of catalysis, including reaction kinetics, simple reactor design concepts, and catalyst preparation, characterization, and deactivation. Accompanying each chapter are questions and suggested readings. Chapters 6–15 describe by category applications and practice in the industry, including process chemistry, conditions, catalyst design, process design, and catalyst deactivation problems for each catalytic process. Chapter 6 describes hydrogen and syngas generation processes for different end applications. Processes for the synthesis of ammonia, methanol, and hydrocarbon liquids (Fischer–Tropsch process) are presented in Chapter 7. Processes for selective catalytic oxidation to (a) commodity chemicals, including nitric, cyanic, and sulfuric acids, formaldehyde, and ethylene oxide, and (b) specialized products such as acrylic acid, maleic anhydride, and acrylonitrile are presented in Chapter 8. Catalytic processes for hydrogenation of vegetable oils, olefins, and functional groups for highly specialized products are presented in Chapter 9. Catalytic processes in refining of petroleum to fuels are presented in Chapter 10. Selected commercial processes utilizing (a) homogeneous catalysts, (b) commercial enzymes, and (c) polymerization catalysts are described in Chapter 11. Chapters 12, 13, and 14 summarize features of important processes for catalysts used in environmental control of gaseous emissions from (a) stationary sources (e.g., power plants) and mobile sources, including (b) gasoline- and (c) diesel-fired vehicles. The final chapter 15 gives a brief summary of (1) catalytic processes for production of bio diesel and ethanol fuels from edible biomass which will ultimately find application to production of similar fuels from non-edible cellulosic biomass and (2) catalyst technology for the emerging hydrogen economy with emphasis on fuel cell technology.

*New York, New York*  
*Iselin, New Jersey*  
*Provo, Utah*  
*22 November 2015*

Robert J. Farrauto  
Lucas Dorazio  
Calvin H. Bartholomew

---

## ACKNOWLEDGMENTS

Drs. Farrauto and Dorazio acknowledge BASF (and Engelhard) for their strong leadership in the field of catalysis. We also acknowledge our students at Columbia University and NJIT, respectively, who have provided course and teaching evaluations that have been invaluable in showing us the need for a simple approach to catalysis and industrial processes.

Dr. Bartholomew is grateful for the financial support of his research, teaching, and writing endeavors by Brigham Young University and of his research by DOE, NSF, GRI, and many companies. He wishes to acknowledge the opportunity to work with distinguished colleagues and friends on the Faculty (especially in the Chemical Engineering Department and Catalysis Laboratory) and some 200+ bright, creative, hardworking graduate and undergraduate students and postdoctoral fellows who worked with him under his direction at BYU. He has also enjoyed the stimulation of teaching more than 750 company professionals during dozens of short courses on catalysis, deactivation, and Fischer–Tropsch synthesis. He wishes to acknowledge the collaboration with and friendship of Dr. Robert Farrauto over the past 42 years, first at Corning Glass, then on a landmark paper, and now two books addressing industrial catalytic processes; he is especially grateful for Bob's patience with him during the long process of preparing the first and second editions of *Fundamentals of Industrial Catalytic Processes*.



---

# LIST OF FIGURES

## Chapter 1

- Figure 1.1 Catalyzed and uncatalyzed reaction energy paths illustrating the lower energy barrier (activation energy) associated with the catalytic reaction compared with the noncatalytic reaction 2
- Figure 1.2 Illustration of catalyzed versus noncatalyzed reactions 2
- Figure 1.3 Catalytic Fe–Ce redox reaction catalyzed by Mn 3
- Figure 1.4 Activation energy diagram for (a) noncatalytic thermal reaction of CO and O<sub>2</sub> and (b) the same reaction in the presence of Pt. Activation energy for the noncatalyzed reaction is  $E_{nc}$ . The Pt-catalyzed reaction activation energy is designated  $E_c$ . Note that heat of reaction  $\Delta H$  is the same for both reactions 4
- Figure 1.5 Conversion of CO versus temperature for a noncatalyzed (homogeneous) and catalyzed reaction 5
- Figure 1.6 Particulate catalysts for fixed bed reactors: spheres, extrudates, and tablets. Powdered catalysts for batch slurry phase processors. A cartoon of a fixed bed reactor loaded with catalyst tablets 9
- Figure 1.7 Adsorption isotherm ( $\theta_{CO}$ ) for CO on Pt for large, moderate, and low partial pressures of CO. The slope at low partial pressures of CO equals the adsorption equilibrium constant  $K_{CO}$  12
- Figure 1.8 Illustration of Langmuir–Hinshelwood reaction mechanism 13
- Figure 1.9 Illustration of Mars–van Krevelen reaction mechanism 14
- Figure 1.10 Illustration of Eley–Rideal reaction mechanism 14
- Figure 1.11 L–H kinetics applied to increasing  $P_{CO}$  at constant  $P_{O_2}$ . Maximum rate was achieved when an equal number of CO molecules and O atoms are adsorbed ( $\theta_O = \theta_{CO}$ ) on adjacent Pt sites 16
- Figure 1.12 Ideal dispersion of Pt atoms on a high surface area Al<sub>2</sub>O<sub>3</sub> carrier 17
- Figure 1.13 Illustration of the sequence of chemical and physical steps occurring in heterogeneous catalysis 20
- Figure 1.14 Conversion versus temperature profile illustrating regions for chemical kinetics, pore diffusion, and bulk mass transfer control 21
- Figure 1.15 Relative rates of bulk mass transfer, pore diffusion, and chemical kinetics as a function of temperature. Chemical kinetics controls the rate between temperatures A and B. Pore diffusion controls from B to C temperatures, while bulk mass transfer controls at temperatures greater than C 22
- Figure 1.16 Reactant concentration gradients within a spherical structured catalyst for three regimes controlling the rate of reaction 23

## Chapter 2

- Figure 2.1 (a) SEM of  $\gamma$ - $\text{Al}_2\text{O}_3$  (80,000 $\times$  magnification) and (b) SEM of  $\alpha$ - $\text{Al}_2\text{O}_3$  (80,000 $\times$  magnification) 33
- Figure 2.2 Three zeolites: (a) mordenite, (b) ZSM-5, and (c) Beta 36
- Figure 2.3 Ceramic and metallic (center image) monoliths of different shapes and cell geometries 41
- Figure 2.4 Ceramic washcoated monoliths 44

## Chapter 3

- Figure 3.1 (a) Adsorption isotherm for nitrogen for BET surface area measurement. (b) Linear plot of the BET equation for surface area measurement. (c) Nitrogen adsorption/desorption isotherm for pore size measurement 50
- Figure 3.2 Mercury penetration as a function of pore size of catalyst 52
- Figure 3.3 Differential porosimetry for a porous catalyst 52
- Figure 3.4 Particle size measurement using laser light scattering analysis 53
- Figure 3.5 Thermal gravimetric analysis and differential thermal analysis of the decomposition of barium acetate on ceria 55
- Figure 3.6 Electron microprobe showing a two-washcoat-layer monolith catalyst. The top layer is Rh on  $\text{Al}_2\text{O}_3$  and the bottom layer is Pt on  $\text{Al}_2\text{O}_3$  57
- Figure 3.7 SEM of  $\gamma$ - $\text{Al}_2\text{O}_3$  with its highly porous network 58
- Figure 3.8 X-ray diffraction patterns of  $\gamma$ - and  $\alpha$ - $\text{Al}_2\text{O}_3$  59
- Figure 3.9 (a) Chemisorption isotherm for determining surface area of the catalytic component. (b) Pulse chemisorption profiles for the dynamic chemisorption method 60
- Figure 3.10 Transmission electron micrograph of Pt on  $\text{TiO}_2$  61
- Figure 3.11 Transmission electron micrograph of Pt on  $\text{CeO}_2$  62
- Figure 3.12 X-ray diffraction profile for different crystallite sizes of  $\text{CeO}_2$  63
- Figure 3.13 An XPS spectrum of various oxidation states of palladium on  $\text{Al}_2\text{O}_3$  64
- Figure 3.14 NMR profile of a Y faujasite zeolite 65
- Figure 3.15 DRIFT spectra of CO chemisorbed on different precious metal particles of catalysts prepared in different ways. The CO chemisorption followed by FT-IR measurements was performed at room temperature after the catalysts were treated at 400  $^\circ\text{C}$  for 1 h with 7%  $\text{H}_2$  in Ar gas 66

## Chapter 4

- Figure 4.1 Illustration of the three processes that can limit the reaction rate during heterogeneous catalysis 70
- Figure 4.2 Illustration showing how experimental rate measurements can be plotted in order to determine the concentration dependence used in the power rate law 74
- Figure 4.3 Illustration showing how experimental rate measurements can be plotted in order to determine the activation energy and pre-exponential factor used in the Arrhenius expression 75

- Figure 4.4 Conversion versus temperature at different space velocities. Experiment is performed to determine the rate constant at various temperatures 76
- Figure 4.5 Arrhenius plot for determining activation energies 83

## **Chapter 5**

- Figure 5.1 Idealized cartoon of perfectly dispersed Pt on a high-surface  $\gamma$ -Al<sub>2</sub>O<sub>3</sub> 89
- Figure 5.2 Conceptual diagram of sintering of the catalytic component on a carrier 90
- Figure 5.3 TEM of fresh and sintered Pt on Al<sub>2</sub>O<sub>3</sub> in an automobile catalytic converter application. "Black dots" are platinum crystallites. The size difference in crystallites between the two pictures is the result of sintering 90
- Figure 5.4 Idealized conversion versus temperature for various aging phenomena 91
- Figure 5.5 Illustration of the sintering of the catalyst carrier occluding the catalytic component 92
- Figure 5.6 Microscopy images of low surface area rutile (a) and high surface area anatase (b). Each set of four photos show the structure at increasing magnification 93
- Figure 5.7 (a) NMR profile of a thermally aged zeolite showing the loss of the Si–O–Al bridges. Si(3Al), Si(2Al), and Si(Al) are seen to decrease in intensity with the progressively more severe thermal aging. (b) Growth of penta- and octahedral coordination sites in a thermally deactivated zeolite 94
- Figure 5.8 Conceptual cartoon showing selective poisoning of the catalytic sites 96
- Figure 5.9 Conceptual cartoon showing masking or fouling of a catalyst washcoat 97
- Figure 5.10 XPS spectrum of the surface of a contaminated Pt on Al<sub>2</sub>O<sub>3</sub> catalyst 98
- Figure 5.11 Electron microprobe showing the deposition location of the poisons within the washcoat of a monolith catalyst used in an automobile catalytic converter. The X-ray beam is scanned perpendicular to the axial direction through thickness of the washcoat 98
- Figure 5.12 TGA/DTA in air of coke burn-off from a catalyst 100
- Figure 5.13 TGA/DTA profile for desulfation of Pd on Al<sub>2</sub>O<sub>3</sub> catalyst 100

## **Chapter 6**

- Figure 6.1 Illustration of industrial hydrogen generation process 105
- Figure 6.2 A series of metallic tubes filled with particulate catalysts bathed in a furnace of burning natural gas providing the required heat of reaction. The rate of reaction and temperature are highest near the heat source 108
- Figure 6.3 Reduction or activation of Ni SR catalyst: H<sub>2</sub>O (steam)/H<sub>2</sub> as a function of temperature for redox of NiO/Ni 109
- Figure 6.4 H<sub>2</sub>O/C versus temperature: a high H<sub>2</sub>O/CH<sub>4</sub> ratio allows higher temperatures for coke-free operation. To the right of the line is the coke forming regime 110
- Figure 6.5 WGS equilibrium: free energy and equilibrium constant for WGS as a function of temperature 114
- Figure 6.6 Typical performance of a HTS WGS catalyst with respect to exit CO 115
- Figure 6.7 Reformer schematic for pure H<sub>2</sub> 118

- Figure 6.8 Overall process flow diagram for preformed natural gas to  $H_2$  and  $N_2$  for  $NH_3$  production 119
- Figure 6.9 Monolith catalysts for  $H_2$  generation using PSA or PROX 123
- Figure 6.10 Illustration of a highly simplified catalyzed double pipe heat exchanger where a combustion catalyst is applied to the inside surface and a steam reforming catalyst is applied to the outside surface of the inner tube 124
- Figure 6.11 Preferential oxidation of 0.5% CO using a (Pt, Fe, Cu)/ $Al_2O_3$  monolith catalyst 125
- Figure 6.12 Various catalytic processes for generating  $H_2$  and synthesis gas from desulfurized natural gas (methane) and methanol 127

## Chapter 7

- Figure 7.1 Simplified flow sheet for  $NH_3$  synthesis illustrating a “quench”-type ammonia converter and two-stage feed gas compression 130
- Figure 7.2 Simplified illustration of a single-stage radial flow ammonia converter 134
- Figure 7.3 Illustration of methanol quench reactor design 136
- Figure 7.4 Illustration of staged cooling design 137
- Figure 7.5 Illustration of cooled tube reactor design 138
- Figure 7.6 Illustration of shell-cooled reactor design 138
- Figure 7.7 Flow sheet for methanol synthesis 139
- Figure 7.8 Bubble slurry reactor for Fischer–Tropsch 142
- Figure 7.9 Loop reactor for Fischer–Tropsch 144

## Chapter 8

- Figure 8.1 Surface roughening (sprouting of PtRh gauze) 148
- Figure 8.2 High-pressure  $NH_3$  oxidation/ $HNO_3$  plant with Pd getter gauze 149
- Figure 8.3 An expanded view of the reactor containing the stacks of oxidation and getter gauzes 150
- Figure 8.4 HCN process flow diagram 153
- Figure 8.5 The Claus process with staged reaction and liquid sulfur removal 154
- Figure 8.6 Elemental sulfur is reacted with dry air at  $900^\circ C$  producing  $SO_2$ . Staged air injection into the second and third stages for cooling is shown in Figure 8.8 156
- Figure 8.7  $SO_2/SO_3$  equilibrium as a function of temperature 157
- Figure 8.8 Quench reactor for  $SO_3$  production with staged air injection for cooling for stages 2 and 3 158
- Figure 8.9 The  $O_2$  process for ethylene oxide production 161
- Figure 8.10 Process for low methanol concentration process to formaldehyde over a (Fe, Mo)/ $SiO_2$  catalyst 162
- Figure 8.11 Process using Ag catalyst 163
- Figure 8.12 Propylene to acrolein to acrylic acid process flow diagram. Tubular reactor with a diameter of about 2.5 cm and a length of about 4 m cooled by a molten carbonate 165
- Figure 8.13 Process for converting propylene to acrylonitrile 167

**Chapter 9**

- Figure 9.1 Illustration comparing difference between a semibatch stirred tank reactor and a continuous stirred tank reactor 172
- Figure 9.2 Illustration of a semibatch stirred tank reactor (STR). The sparger (or also called dip tube) is used for continuous addition of a reactant, which is hydrogen for hydrogenation reactions. Not shown is the removal of unreacted hydrogen from the headspace, which must occur to maintain the desired reactor pressure 173
- Figure 9.3 Illustration showing hydrogen consumption versus time during typical hydrogenation reaction 173
- Figure 9.4 Illustration of the mass transfer path taken by hydrogen as it diffuses from the gas bubble, through the bulk liquid, and ultimately to the catalyst particle. In most hydrogenation reactions, the rate of this diffusion process limits the overall rate of reaction 174
- Figure 9.5 Kinetic rate for a catalytic slurry-phase batch reaction 176
- Figure 9.6 Linolenic oil shown as an example of an unsaturated fat molecule 178
- Figure 9.7 Sequential reactions at 140 and 200 °C 179
- Figure 9.8 CATOFIN propane dehydrogenation to propylene using  $\text{Cr}_2\text{O}_3/\text{Al}_2\text{O}_3$  catalyst 185
- Figure 9.9 Flow diagram for dehydrogenation of ethyl benzene to styrene 187

**Chapter 10**

- Figure 10.1 Simplified illustration of the crude oil refining process. The desalting process (removal of inorganic components in the crude using a water wash) is not shown 192
- Figure 10.2 Examples of metal-containing (nickel porphyrin) and sulfur-containing (thiophene) species typically found in crude oil 193
- Figure 10.3 The HDM/HDS process flow diagram. Inset shows presulfided catalyst and its positive effect on decreasing excessive gas make and hydrogen consumption 195
- Figure 10.4 Catalyst deactivation by HDM metal deposition (masking) and coking 196
- Figure 10.5 Controlled  $\text{O}_2$  addition in coked catalyst regeneration 196
- Figure 10.6 Faujasite zeolite 198
- Figure 10.7 Schematic of FCC reactor with catalyst regenerator 199
- Figure 10.8 Process flow diagram for naphtha reforming 201
- Figure 10.9 Regeneration and rejuvenation of  $(\text{Pt}, \text{Re})/\gamma\text{-Al}_2\text{O}_3 + \text{Cl}^-$  reforming catalyst 202

**Chapter 11**

- Figure 11.1 Hydroformylation process using a cobalt homogeneous catalyst 207
- Figure 11.2 Dow (Davy McKee) LP Oxo Selector process using the Rh catalyst 207
- Figure 11.3 Monsanto acetic acid process 209
- Figure 11.4 Phillips loop reactor 211
- Figure 11.5  $\text{TiCl}_3/\text{MgCl}_2$  process for polyethylene 212



**Chapter 12**

- Figure 12.1 (a) VOC abatement process with heat integration. (b) VOC abatement with supplemental heating 223
- Figure 12.2 Slipstream reactor concept used for VOC abatement design 224
- Figure 12.3 Catalyst abatement of food processing fumes 225
- Figure 12.4 SCR with  $V_2O_5$  and a metal-exchanged zeolite: 1.1  $NH_3/NO$  and zeolite 228
- Figure 12.5 SCR reactor schematic. It would be worth mentioning that the widening, that is, lower velocity, increases contact time 229
- Figure 12.6 Ozone abatement reactor design 230

**Chapter 13**

- Figure 13.1 Gasoline-relative engine emissions and temperature as a function of air/fuel ratio 236
- Figure 13.2 Monolith catalyst housed in a metal canister secured in the exhaust 239
- Figure 13.3 Optical micrographs of double-layered washcoated ceramic monoliths 243
- Figure 13.4 Conversion proceeding axially down the channel of a monolith with poisoning. Units of time are arbitrary units 249
- Figure 13.5 Temperature profiles ( $\Delta T/\Delta L$ ) for an exothermic reaction down the axial length of a catalyzed monolith channel caused by sintering 250
- Figure 13.6 Simultaneous conversion of HC, CO, and  $NO_x$  for TWC as a function of air/fuel ratio 252
- Figure 13.7 Oxygen sensor response output as a function of air/fuel ratio 253
- Figure 13.8 Electron microprobe scan of an automotive catalyst contaminated with P and S from lubricating oil 255
- Figure 13.9 Close-coupled TWC catalyst, under-floor TWC, and oxygen sensors connected to electronic feedback to control air/fuel ratio close to stoichiometric ( $\lambda = 1$ ) 258

**Chapter 14**

- Figure 14.1  $NO_x$ -particulate trade-off with emission regulations 263
- Figure 14.2 Electron microprobe scans of the washcoat of an aged diesel oxidation catalyst. (a) Zn and Ca. (b) P and S 266
- Figure 14.3 Wall flow filter. Soot particulates deposit on the porous wall, while the gaseous components ( $CO_2$ ,  $H_2O$ ,  $NO$ , and  $NO_2$ ) and air pass through. The soot is combusted periodically by raising the inlet temperature to  $>500^\circ C$  when a small amount of diesel fuel is injected into the DOC 267
- Figure 14.4 SCR with Cu and Fe zeolites 268
- Figure 14.5 Schematic of simplified diesel exhaust aftertreatment system. A diesel oxidation catalyst and wall flow filter (or diesel particulate filter) are contained in one canister, a dosing system for injecting urea to the SCR catalyst. An ammonia decomposition catalyst ( $Pt/\gamma-Al_2O_3$ /ceramic monolith) is installed at the outlet of SCR. The DOC catalyzes the oxidation of CO, HC, and some of the NO to  $NO_2$  and generates sufficient heat ( $\sim 500^\circ C$ ) by oxidizing injected diesel fuel to initiate combustion of the soot collected on